

# Systematic Studies on Building the High Output Thermoelectric Power Generation

Anjun Jerry Jin<sup>1,2,\*</sup>, Yuanming Zhang<sup>2</sup>

<sup>1</sup>Acad. of Sciences, on Leave from the Solar Thermal Energy Division, China Huaneng Clean Energy Research Institute, Huaneng Innovation Base Laboratory Bldg-A FutureTech City, Beijing, China

<sup>2</sup>Ningbo Inst. of Industrial Technology, Acad. of Chinese Science, Ningbo, China

## Email address:

ajjin@hnceri.com (A. J. Jin), zhangwolfson@qq.com (Yuanming Zhang)

\*Corresponding author

## To cite this article:

Anjun Jerry Jin, Yuanming Zhang. Systematic Studies on Building the High Output Thermoelectric Power Generation. *International Journal of Science, Technology and Society*. Vol. 5, No. 4, 2017, pp. 112-119. doi: 10.11648/j.ijsts.20170504.19

**Received:** May 14, 2017; **Accepted:** May 31, 2017; **Published:** July 12, 2017

---

**Abstract:** Authors report a systematic approach in research and development of alternative energy with a focus on thermoelectric (TE) generation. This approach has improved the thermoelectric modules (TEM) and thermoelectric power generator (TEPG) system in the key specification. In particular, they have investigated the details of the TE technology, constructed TEM, and built TEPG in order to achieve large power output and high efficiency. Experimental studies of the in situ characterization station for the thermoelectric module (ICSTEM) discover that the multi stack TEM has significantly improved the efficiency of a system by employing suitable and commensurate TE materials. The ICSTEM is invented to establish precisely a true TEM performance. Typical electrical response curves are studied in terms of IV curve and PV curve. This article has also characterized the output power as a function of the force factor setting and of its demonstrated response curve. Moreover, by connecting various TE prototypes, the total power output shows the scalability by simple superposition. Finally, authors demonstrate the TE device manufacture by the different approaches of advanced manufacturing technologies and explore ways of advanced manufacturing processes.

**Keywords:** Renewable Energy, Energy Harvesting, Thermoelectric Generation, Multi Stack, Smart Grids

---

## 1. Introduction

There are intense interests in the development of the alternative energies [1-2]. Extensive studies are conducted both theoretically and experimentally [3-5] on the promising solid-state solar thermal electric generation. Moreover, there are extensive researches recently dedicated to study the thermoelectric power generation (TEPG) in producing power ranges from small to large. In contrast to the solar technology that has solar panels collect photon energy and convert it into electricity, a very different type of renewable energy (RE) technology is TEPG that converts heat into electricity. TEPG with thermoelectric modules (TEM) generates energy from renewable energy sources such as solar, geothermal, fire source, and other heat sources like waste heat/energy harvesting. The thermoelectric (TE) energy is advantageous as RE in many ways, including in part being noiseless with

no moving parts, light weight, no need or little need for maintenance. The current work endeavors to advance TEPG technology.

To apply a foundation in TEPG, the governing laws of physics is the Seebeck effect [6]. The TE device can be understood by a simplified illustration of the Seebeck effect as follows: it converts thermal energy directly into electrical energy and typically employs a pair of dissimilar TE materials to make a device. The output voltage  $\Delta V$  of a TE device generally increases with the temperature differential  $\Delta T$  linearly as follow. In a combination of N-type and P-type materials,  $\Delta V \cong S_{NP} \cdot \Delta T$ ; where the constant, called the Seebeck coefficient ( $S_{NP}$ ), is related to the materials properties (pairs).

In addition to the efficiency of TEM and/or TEPG, the

output power level is another important factor. The power level can be achieved through the integration of a large number of TE devices, the efficiency is determined by temperature differential and by a dimensionless figure of merit  $ZT$ .  $ZT$  is characterized by several material parameters such as the Seebeck coefficient ( $S$ ), thermal conductivity, and electrical resistivity [7-9]. The total power output equals the total heat input multiplied by the efficiency. In the later section(s), authors will show that the properties of most TE semiconductors depend upon temperature, e.g., a single TE material typically operates well in about a couple of hundred degrees of temperature window [10].

There are numerous applications for TEPG ranging from the bio-thermoelectric to the deep-space power supplies. For example, TEPG delivers key power supply with radioisotope enabled TE output, which delivers 350W for the Appolo mission to the Mars. In view of the technological pain, the author has studied the pain points in the industry and has highlighted some challenges in this article. If TEM/TEPG must be economical, one significant factor is that the efficiency should achieve some system level, e.g., with a figure of merit,  $ZT \geq 2$ . For example, an efficient TE product will in general help keeps costs down and stay competitive.

Finally, based on the research project of a systematic study, the article will cover the following reports: illustrate the experimental setup, measure data, analyze and understand the implication, discuss results, and draw conclusions.

## 2. Systematic Studies

Systematic studies of the TE system are reported as follows.

### a. Experimental Setup

To start an experimental discussion, a thermoelectric module is a circuit module that contains a large number of thermoelectric devices fitted together to generate a significant amount of output power. The setup of an operating TE generator includes multiple levels of a TE system hierarchy as follows. A TE device is typically composed of two dissimilar TE legs as illustrated in Fig. 1a). The temperature differential causes a net current in the P- and N- type TE legs. A typical TEM integrates a large number of TE devices shown in Fig. 1b). The heat flows through the temperature difference across the device. As devices are connected either in serial, in parallel, or in combination circuit per design, the thermal energy generates a total electromotive force across the two electrical leads Fig. 1b) as shown. Fig. 1a) and Fig. 1b) illustrate the principles of the TE device operations.

A variation of the TE system depends on technological applications; e.g., some interesting illustration may refer to reference [11]. When TEPG is built, researchers have applied careful thermal management methods and built systems at various power levels. The methods include the fine insulation mentioned to be shown later in this section, and good uniformity conducting heat [for both the cooling surface and heating surface]. The hot side normally employs one of the

heating choices of the infrared heat, of fire-heat, of electric heaters, of solar thermal, or of liquefied natural gas (LNG), and other methods. The LNG is normally warmed to be used in cooking as well as electricity generation and other uses. The above choices are laid to establish the groundwork prototypes for various (potential) applications.

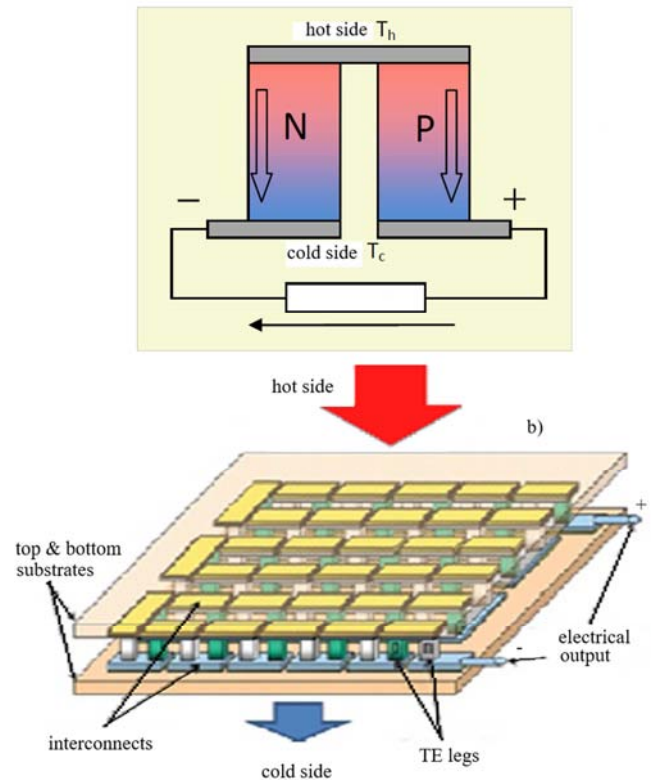


**Figure 1.** 1a) a schematic illustrates a basic TE device where after its p- and n-type TE elements are under temperature differential; an electromotive force is generated. 1b) TEM is an integration of TE devices connected to provide an increased power output.

The in situ characterization station for the thermoelectric module (ICSTEM) is an instrument to measure in situ the conversion efficiency of TEM. It is comprised of the following tests: measure the output power  $P$ , current  $I$ , inner resistance  $R$  and the cold end heat flux  $Q_c$  of the thermoelectric module under power generation status. The efficiency is defined as the ratio of the electric power output,  $P$ , to the heat input,  $Q_h$ , on the hot side of the thermal electric device.

The ICSTEM is carefully designed so that the physics of heat flow can be well-described by that of the heat flux which flows through the z-direction and that the thermoelectric conversion efficiency can be measured conveniently in situ in real time. Theoretically, the cooling capacity  $Q_c$  is calculated as follows:

$$Q_c = S_{NP} T_c I - \frac{1}{2} I^2 R - k(T_h - T_c)$$

Where  $S_{NP}$  is a TEM Seebeck coefficient;  $T_h$  and  $T_c$  are its temperature at hot side and cold side, respectively;  $I$  the current,  $R$  the resistance, and  $k$  the thermal conductance. The cooling capacity is maximal when a TEM has the same cold-

side and hot-side temperatures.

When the ICSTEM is designed [7], TEM should be placed flat and be parallel with the two relative edges of the heat flux sensors near its cold side. Referring to Fig. 2, the flat surface of the cold plate can be vertically adjusted by the four setscrews independently; each set screw has a fine threaded resolution of ten microns and below. The torque pressure can be set on the flat surface via the torque wrench as shown which could guarantee the peak level TE performance. Fig. 3 illustrates a typical four-point probe that measures the efficiency of TE device/legs in an open-air condition. A temperature differential is applied from both of the designated top- and bottom-plates. The actual temperatures on every side are measured in real time with two thermocouples (TCs). The efficiency is measured as a function of temperature. I-V and P-V features will be investigated later.

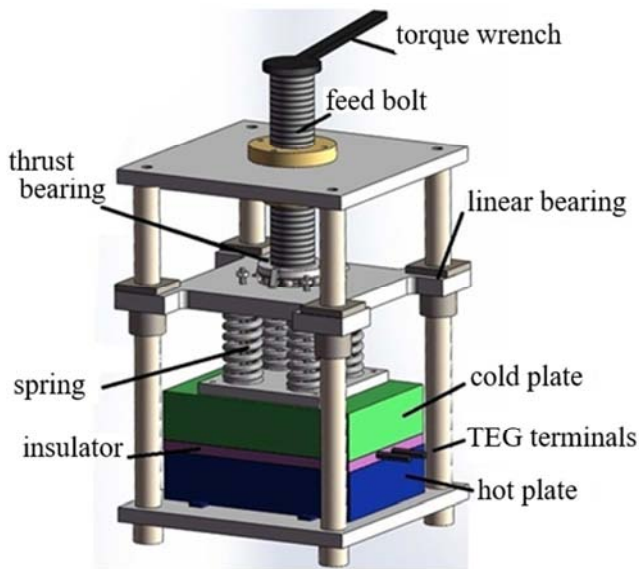


Figure 2. ICSTEM schematic illustrates the TEG sandwiched by the cold plate and hot plate where the efficiency is measured in situ.

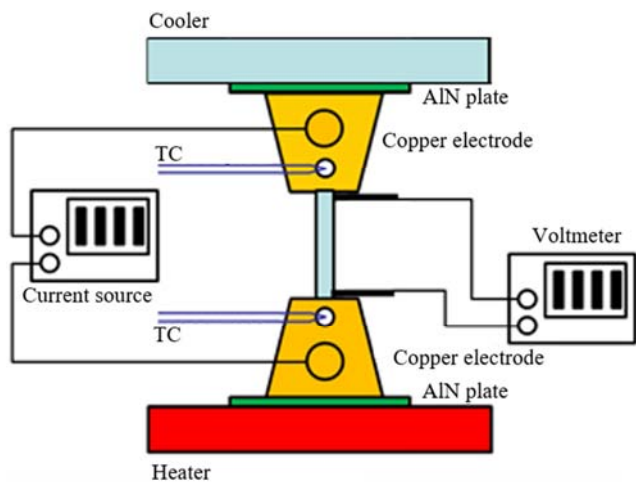


Figure 3. The schematic is a four-point probe to measure I-V curves of TE pairs. The electrical current and the voltage across TE leg is measured by the meters. Copper and/or AIN are employed for the best contact either electrically and/ or thermally.

The system has relatively small size, is thermally insulated at peripheral surfaces, and has good uniformity conducting heat to the cold and hot surfaces. The hot side controls the temperature  $T_h$  with specific heat source; the cold side controls temperature  $T_c$  of the thermoelectric module undercooling conditions. In this case, the cold side employs one of cooling choices [e.g., water, or liquid nitrogen cooled]. High infrared reflection and insulation materials, for example, may be chosen as the alternating layers of thin metal sheet and thin glass fiber sheet [or insulator layer]. This can significantly reduce the influence of the heat leakage in heat conduction. The in situ characterization station is carefully designed so that the physics of heat flow can be well described by a 1D heat flow model [12] that the heat flux flows through the z-direction.

b. Analysis and Data Collection

Many studies are conducted on TEM and TEPG system(s) and characterized in this article. When  $T_h$  reaches  $300^\circ\text{C}$ , the output power has reached 300W or more per unit; it exceeds 1000W with a group of four units. Researchers have designed, first built, and tested in the laboratory as well as tested in the field. The prototype has delivered the output power that is predicted by simulation results. The simulation model has been conducted utilizing SolidWorks® [13] thermal physics software with a proprietary algorithm.

A number of heat sources and/or cooling mechanism are employed to the various extent of success to demonstrate a range of TEPG power output. Author have investigated many options as follows. For example, the infrared heating is used as a heat source, the direct-fired diesel burner employed, or the LNG burner employed as well.

The output power is plotted in the figure as a function of the hot side temperature. Moreover, a range of heat sources from the automotive tailpipe energy harvesting to a solar heater is employed for the investigation.

Fig. 4 illustrates the relationship of power output and temperature built and tested with commercial TE modules [14]. Based on the combined multiple unit studies, the total power output is superimposed well in either serial or parallel configuration and typically equals to the sum of all units of individual TEPG [11].

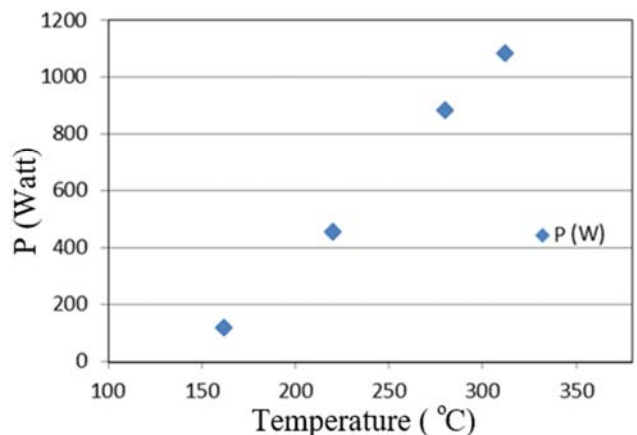


Figure 4. Lab tests for the power output of TEPG show that its maximum output depends nearly linearly upon the temperature in the tested range.

The TE efficiency is demonstrated in Fig. 5; it shows the relationship of TE efficiency as a function of the hot side temperature. It is expected that the efficiency increases with the temperature. Moreover, many tests for different modules covering various temperature ranges have been demonstrated and overlaid in the same figure. In addition to the nearly linear relationship of the efficiency vs temperature, TE devices have exhibited TE efficiency from a few percent to ten percent. The TE efficiency of the dual stack is approximately ten percent and lies above this chart. The dual stack efficiency lays above the chart at 450°C. Further studies on details of the Efficiency vs temperature relationship are in progress.

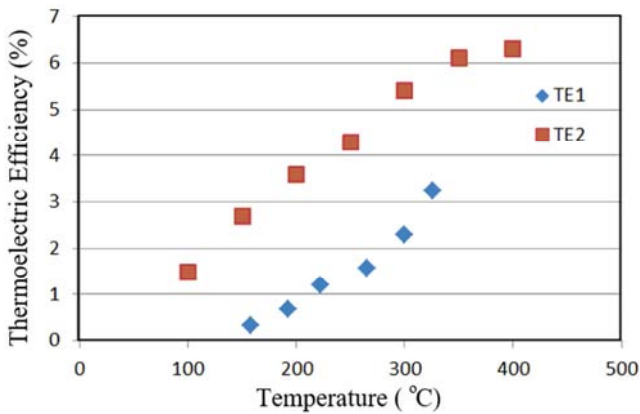


Figure 5. The charts demonstrate the dependence of efficiency versus temperature at their hot side of TE systems [14]. TE1 and TE2 studies the efficiency of off-the-shelf sample-1 and sample-2, respectively.

c. Discussions of TE Stacks

The experiments & investigations are undertaken as follows.

Fig. 6 illustrates the dependence of efficiency upon the length ratio (x) for both P-type and N-type TE materials, where x is the joint position in the ratio of the length where segmented legs locate it. Fig. 6a) shows P-type efficiency as a function of x at three temperature settings; Fig. 6b) shows N-type as a function of x. The TE efficiency is 11.8% at 550°C, Th, for P-type; and it is 9.7% at 550°C for N-type

In Fig. 7, each TEM device is characterized for its fundamental electrical property traces in terms of current (I) versus voltage (V) curves, i.e., I-V curves, and in terms of power output [at maximum value point] P versus V, i.e., P-V curves. Figures have plotted typical data of a system at three different temperature settings at the hot side as follows. Fig. 7a) shows I-V curves exhibiting typical electrical traces of a low resistance power supply, and Fig. 7b) shows P-V curves of typical resistance power traces. The power output increases with the temperature  $T_h$ .

The empirical analysis based on the data at above, generally concurs with results derived from the SolidWorks® model [13]

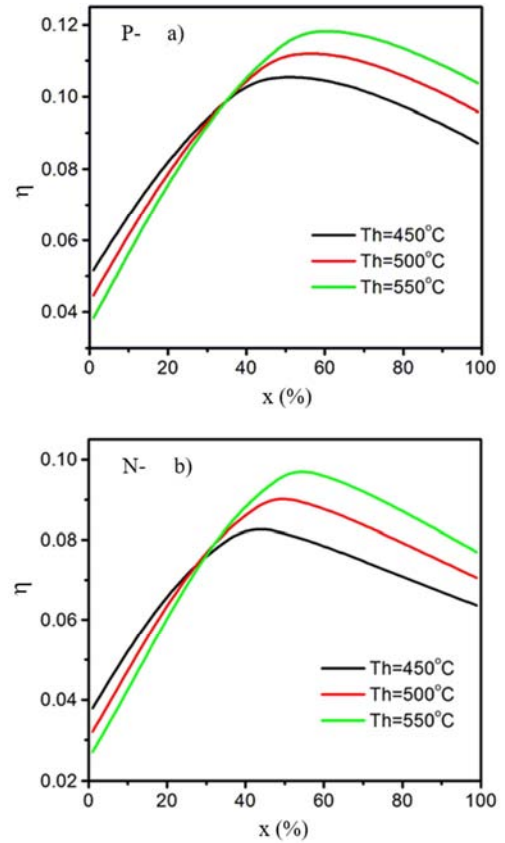


Figure 6. Illustrates efficiency for both P-type and N-type materials. 6a) P-type efficiency is exhibited as a function of x at 3 different temperature settings; 6b) N-type efficiency as a function of x at 3-settings.

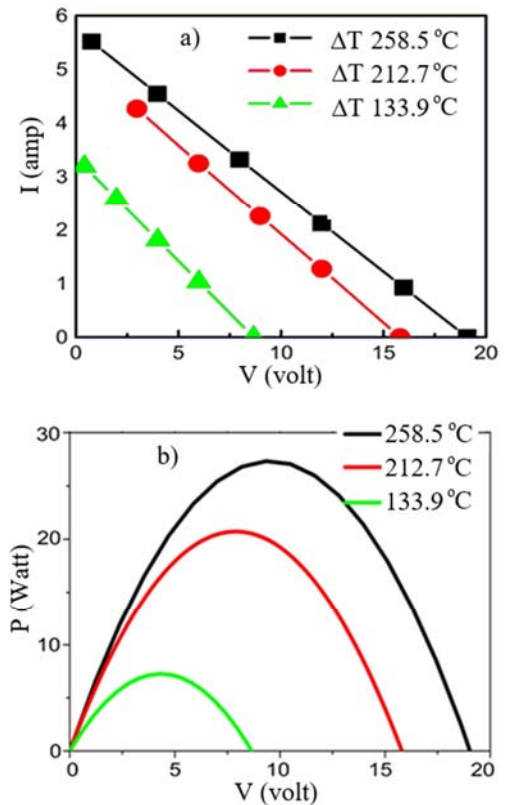


Figure 7. 7a) I-V curves exhibit typical features of a resistive power supply; 7b) P-V curves show typically resistive feature.



d. Results and Discussion

The TEM is built in the laboratory. It can produce electricity, which is demonstrated at various output specs up to 1kW level with wide choices of heat sources.

Researchers have built multi stack with the available TE materials. The computer simulation with the finite element method of triple stack TEPG predicts that the efficiency can achieve over 19% [15].

This article shows that the dual stack system is built and has achieved 10% efficiency in the lab. Conversion of the thermal energy into electricity employs solid-state devices that has no moving parts, and expands the use of the energy resources vastly. Similar to other distributed power or RE power plants, TEPG is an environment that is also beneficial and convenient for integration into the smart grid.

In order to achieve improved efficiency and/or power level, the chosen TE materials are optimized suitably for segmented-legs. The TE leg preparation has enabled the superior efficiency of the TEM [16].

As shown in Table I, the dual stack materials consist of PbTe based and BiTe based TE materials. The first types are PbTe based TE materials (and its variation stoichiometry) include both in P-type and in N-type being optimized for a medium temperature range; the BiTe TE materials (and its variation stoichiometry) include both in P-type and in N-type optimized for a low-temperature range.

The dual stack P- and N-type PbTe/ BiTe based segmented legs are joined together at a high temperature through hard soldering that otherwise can not be welded together. The dual stack TE system exhibits the enhancement figure of merit ZT of the system as shown in Table I below. The ZT is tabulated for several TE materials covering high temperature.

Careful studies measure the efficiency of 10% when a temperature differential has reached 400°C. The table employs temperature unit K, where  $m/K = n/C + 273.15$ .

**Table 1.** Figure of merit ZT of TE materials/ legs is tabulated at below: (P\_PbTe:  $Pb_{0.94}Sr_{0.04}Na_{0.02}Te$ , N\_PbTe:  $Pb_{0.94}Ag_{0.01}La_{0.05}Te$ , P\_BiTe:  $Bi_{0.5}Sb_{1.5}Te_3$ , N\_BiTe:  $Bi_2Te_3$ )

| P- PbTe |      | N- PbTe |      | P- BiTe |      | N- BiTe |      |
|---------|------|---------|------|---------|------|---------|------|
| T(K)    | ZT   | T(K)    | ZT   | T(K)    | ZT   | T(K)    | ZT   |
| 321     | 0.17 | 320     | 0.18 | 327     | 0.88 | 326     | 0.83 |
| 422     | 0.48 | 420     | 0.39 | 379     | 0.95 | 373     | 0.94 |
| 522     | 1.13 | 524     | 0.71 | 431     | 0.91 | 423     | 1.11 |
| 622     | 1.76 | 620     | 1.09 | 482     | 0.72 | 524     | 0.92 |
| 722     | 1.86 | 726     | 1.44 |         |      |         |      |
| 822     | 2.12 | 824     | 1.51 |         |      |         |      |
| 922     | 2.05 | 924     | 1.41 |         |      |         |      |

If the unit cost continues to drop from the current price tag of the off-the-shelf TEM, and if  $ZT \cong 2.0$ , TEPG can possibly competitively achieve an advantage in the economies of scale. There are extensive studies to improve ZT with new TE materials in the literature [e.g., 7, 16]. It is the author’s belief that the current TEPG technology is still in the early stage with a limit in TE efficiency attributes of the available materials.

ZT is related to material properties including electrical conductivity, thermal conductivity, and Seebeck coefficient.

With reference to Table I, the favorable working temperature of PbTe based materials is from 573 degree-K to 873 degree-K. The dimensionless figure of merit in the relevant temperature range ( $ZT = S^2/\rho\kappa$ ) is about 1.5~2.1 for P-type and 0.9~1.4 for N-type. The BiTe based TE materials cover the temperature range lower than PbTe. The dimensionless figure of merit in the relevant temperature range is about 0.7~0.9 for P-type and 0.8~1.1 for N-type. The upshot of experimental data is that the multi stack of TEM improves the system TE efficiency.

The Author has achieved hundreds of watts in power output for each TEPG system unit and has produced 1kW by additively connecting a few units together. Moreover, by utilizing the currently available thermoelectric materials and employing dual stack TEMs, the above data demonstrate that the dual stack TEM leads to a higher efficiency than a single stack as expected.

The combined results of multi stack TE materials utilize P\_PbTe, N\_PbTe, P\_BiTe, and N\_BiTe. The discovery includes dual stack TE device of 10% efficiency; computer modeling delivers 19% efficiency for triple stack TEM.

Finally, among rich applications, authors have investigated many important parameters/ conditions as follows: operating pressure setting, in situ efficiency study, and the materials research and TEPG scalability [11]. More work to improve both the efficiency and production cost is in progress.

e. Additivity

The additivity of TEG systems demonstrates the physical scalability and its trends are investigated for TEG systems that work out generally very well. For example, in one case the temperature differential is set at 95°C for two of the TEG prototypes. After taking standard measurements, data were recorded as follows: prototype-A delivers 19.95 Watt; prototype-B delivers 19.45 Watt. The data also show that the total power satisfies the law of additivity. The total power in serial connection of the two systems yields an output of 39.27W and the power in parallel connection of the two systems yields an output of 39.11W. Likewise, the case at 62°C satisfies the additivity, too.

The errors are shown to be insignificant; multiple tests made us conclude with a level of confidence over 99.5% that the superposition meets the law of additivity. The error bar for the power data is very small.

The table II below illustrates the experimental proof of the additivity law. The additivity is reproduced for several tests where each and every one works out precisely. In other words, this is a typical behavior shown in table II.

**Table 2.** Demonstration of power scalability in order to superimpose TEG prototype with typical test data shown at below.

| $\Delta T(^{\circ}C)$ | $P_A$ (W) | $P_B$ (W) | Serial (W) | Parallel (W) |
|-----------------------|-----------|-----------|------------|--------------|
| 62.0                  | 8.98      | 8.22      | 17.00      | 17.07        |
| 95.0                  | 19.95     | 19.45     | 39.27      | 39.11        |

f. Clamping Force

Over a wide range of the force applied, the output power could be very significant. A typical TE module demonstrates the force response curve, which is shown in Fig. 8, as follows.

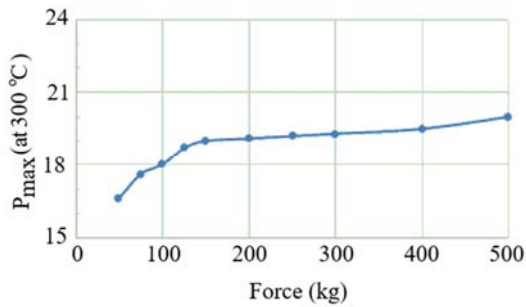


**Figure 8.** Maximum output power curve for a module under different clamping forces, with a cold side of 25°C.

Referring to the chart, the experimental curve is taken, where the hot side temperature is 300°C and the cold side temperature is 25°C.

Researchers discover a typical relationship of TEM output power and the applied clamping force. Near the low force side, the power increases significantly with the force. The curve exhibits a total variation of twenty percent that is also observed in many times at various temperature settings.

As it is shown in the chart, the force chosen at 250kg works well where the curve essentially flattens. Moreover, the clamping force is set below 350kg in order to limit any risks of failure caused by a crack or other defects at very high clamping forces. At a wide temperature window, the 250kg force is a good setting choice for the force which equals to 8.0kg/cm<sup>2</sup> of the experimental pressure setting.

The causes of the chart trends has been believed to do with the defects or factors of contact interface behavior such as variation in electrical contact resistance, air gap, interfacial structures, and changes caused by packaging materials.

The aforementioned defect or imperfection [of TEM] could be optimized through proper setting of the clamping force, and the optimization should reduce extra parasitic losses with optimized setting with low parasitic losses: e.g., low contact resistance, small radiation effects, little inter-diffusion at any junction.

#### g. Applications, Discussions, and Perspectives

There is tremendous commercial potential with the interesting TEPG application. Talele et al. [18] have discussed the solar thermoelectric generation. Their study asserts that ZT, in the range of 2.0 to 3.0, would be extremely appealing in the thermal electric efficiency by applying focused solar technology. This efficiency is approximately on par with the poly silicon solar cells.

In the stated ZT range, Kandantzis group [19] has discovered several new materials, such as PbTeS<sub>0.3</sub>, which exhibits a large ZT. There are other technologies to achieve high efficiency of thermal electric energy conversion. For example, the thermoionic electricity [20] is worthy of remarks. This method can have a significant efficiency that typically operates in the lower temperature range. The multi stacks thermoelectric conversion has attracted many interesting research and development.

Researchers have conducted experiments and have explored prototypes that cover the whole range from 1W to

1000W. Based on the data evidence, the technology can lead to commercial reality with the desired power range, efficiency, and low manufacturing cost.

One of the manufacturing methods is the mature VLSI process in the semiconductor industry. The keys are the pattern etching and TE materials filling for the device circuit [22]. Subtractive processes are investigated as shown in Fig. 9 in details at below. Fig. 9a) shows the patterned oxide insulator in cross-section view; Fig. 9b) shows/ illustrates the filling after p- and n- BiTe; Fig. 9c) is the module after in-house packaging.

Advanced manufacturing technology can advance the TEG and help to reduce costs in applications. In the next section, researchers will explore more of the advanced manufacturing technology. The investigation of BiTe TE modules is carried out by the subtractive VLSI process; where TE devices are embedded in the oxide substrate by the removal of undesired materials to achieve designed device; the size is clearly labelled in the figures. Figs. 9a), 9b), 9c) illustrates the micro-features of etching and filling structure that has TE devices embedded in the oxide substrate. The subtractive VLSI process technology has been reported elsewhere.

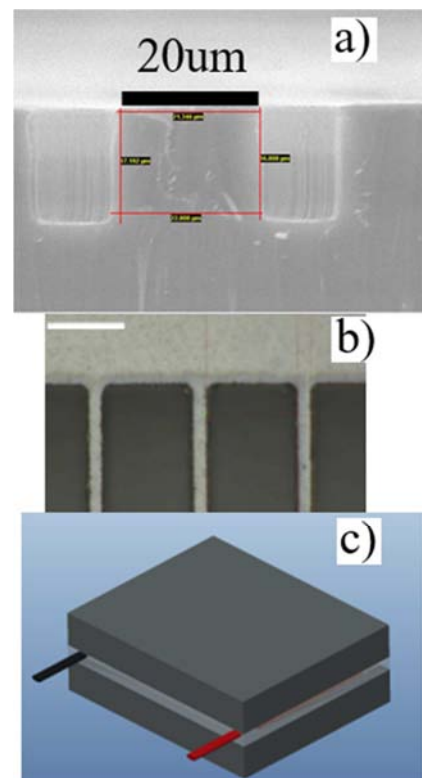


**Figure 9.** Schematics of VLSI process are demonstrated as follows: 9a). cross-section view of etched pattern in oxide film; 9b) filling after p- and n- BiTe materials; 9c) schematic of in-house packaging of a TE module.

#### h. Advanced Manufacturing Technology

Researchers have explored a whole range of large-scale integrated structure of TEM manufacturing processes; both additive manufacturing processes and subtractive VLSI process technology are studied for the TE device manufacturing, respectively.

The additive manufacturing technology grows layers of additive metals/plastics and other materials to deposit all materials according to the design. For example, the micro-jetting process of 3D printing can employ various materials and build up a component in layers.

The micro-jetting process of 3D printing is shown in Fig. 10a), it can be seen that the perfusion of conductive ink in the cartridge instead of the traditional printing inks through ink jet nozzle on a substrate, which controls droplet to directly print out the preset pattern and stack (layer-by-layer) to produce multilayer structures.

The micro-jet technology is an important example of an advanced material manufacturing technology, and it can significantly increase the device and wire density [23]. The micro-jet principle is to use the controllable manufacturing process as shown in Fig. 10a). The technology uses the controllable micro-nozzle to the electronic slurry droplets and to spray desired materials on the substrate surface with the printing nozzle or substrate movement. The material paste droplets will be in the substrate to print the desired circuit pattern and to be fully cured thereafter. The technology can realize the variable resolution superfine linewidth for the complex circuit of the three-dimensional structure, for the production of flexible IC with VLSI [24]. In addition, the technique can be carried out on a non-planar process under a high-speed print with the advantage of less pollution.

Fig. 10b) is the application field and application example of micro jet 3D printing technology; this technology can realize the direct manufacture of the electronic circuit board, the micro-thermocouple, the super capacitor, the logistics tracking mark, the safety wireless shielding antenna and the biochemical sensor, it can also be used in the field of photovoltaic power generation and thermoelectric power generation and other fields to achieve thermoelectric power generation embedded 3D printing.

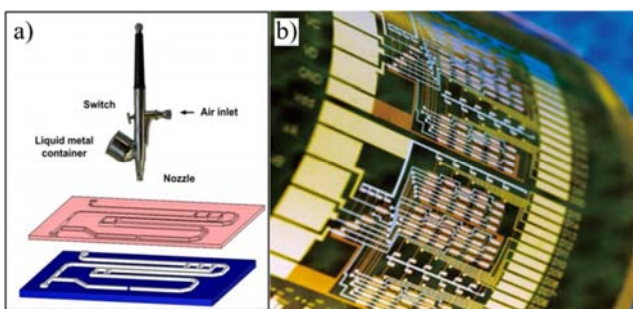


**Figure 10.** The figures show the following: 10a) micro-jet printing illustration; 10b) flexible circuits.

Although the 3D printing technology of flexible electronic devices is still in the stage of research and development at present, it is expected that the technique can change the traditional electronic circuit manufacturing mode, due to the nano-slurry technology can be directly sprayed on the surface of various substrates of nano-slurry without traditional acid corrosion, which can greatly reduce the production cost in small batch production [to meet various commercialization

purposes]. This can bring a profound change to thermoelectric power industry.

#### i. Conclusions

The authors endeavor systematic approaches in the research. They pursue the scientific and technological methodology in building the thermoelectric generation systems.

Many prototypes are built in a wide application range; the output power specs cover over four orders of magnitude up to 1000W. System optimization enables the authors to successfully build many prototypes. They have studied many features of electrical performance of TEPG system.

An advanced platform of in situ measurements is constructed to study the thermoelectric efficiency. Important technologies based on the systematic research are investigated.

Because the materials are often suitable for a limited T-window [about 200°C], a combination of multi-stack TE materials is studied to improve the window. TEM is made via a multi-stack approach that gives superior efficiency of the system. For example, studies show that dual stack PbTe class and BiTe class can achieve 10% efficiency and that, in triple-stacks, the TE device can achieve 19% efficiency. The system scalability and the force factor are identified.

Based on all of the evidence existing in the niche market, the TEPG technology is believed to be on the verge of mainstream applications. The high-quality heat helps to maintain the large temperature differential in order to deliver quality outputs. Various manufacturing processes are studied in the above approaches.

## References

- [1] J. N. Brass, S. Carley, L. M. MacLean, E. Baldwin, "Power for Development: A Review of Distributed Generation Projects in the Developing World". *Annual Review of Environment and Resources*. 37: 107 (2012). doi: 10.1146/annurev-environ-051112-111930.
- [2] "Sustainable Communities Design Handbook: From Green Policy Design, Engineering, Health, to Technologies, Economics, Contracts, Education and Law", Publisher: Elsevier Press, Germany (2015).
- [3] G. Chen, "Theoretical Efficiency of Solar Thermoelectric Energy Generators," *Jnl. of App. Phys.*, Vol. 109, No. 10, pp. 104908-1049088. [May, 2011]. <http://dx.doi.org/10.1063/1.3583182>.
- [4] Y. Deng and J. Liu, "Recent Advances in Direct Solar Thermal Power Generation," *Journal of Renewable and Sustainable Energy*, Vol. 1, No. 5, 2009, ID: 052701. <http://dx.doi.org/10.1063/1.3212675>.
- [5] T. M. Tritt and M. A. Subramanian, "Thermoelectric Materials, Phenomena, and Applications: A Bird's Eye View," *MRS Bulletin*, Vol. 31, No. 3, pp. 188-198 [Jan, 2011]. <http://dx.doi.org/10.1557/mrs2006.44>.
- [6] W. Thomson, "On a mechanical theory of thermoelectric currents", *Proc. Roy. Soc. Edinburgh*: 91–98. (1851).

- [7] J. Mao, Z. Liu, and Z. F. Ren, "Size effect in thermoelectric materials", *npj Quantum Materials* Vol.1, 16028 (Dec, 2016); <http://www.nature.com/articles/npjquantmats201628>.
- [8] D. Liu, Q. Li, W. Peng, L. Zhu, 1 Hu Gao, Q. Meng, and A. J. Jin, "Developing Instrumentation to Characterize Thermoelectric Generator Modules", *Rev. Sci. Instrum* 86, PP703 (2015).
- [9] D. Zhao, C. Tian, S. Tang, Y. Liu, L. Jiang, and L. Chen, "Fabrication of a CoSb<sub>3</sub>-based thermoelectric module", *Materials Science in Semiconductor Processing*, 13, 221–224 (2010).
- [10] DT Crane, D Kossakovski, LE Bell "Modeling the Building Blocks of a 10% Efficient Segmented Thermoelectric Power Generator", *J. Electron. Mater.* 38: 1382-1386 (2009).
- [11] A. J. Jin, W. Peng, Y. Jin, D. Liu, and Q. Li, "Research, Development, and Applications of the High-Power Thermoelectric Generation Technology," *ARPN Journal of Science and Technology*, 3, 901 (2013).
- [12] S. A. Solla and E. K. Riedel for a good 1D heat flow model, "Vortex excitations and specific heat of the planar model in two dimensions," *PhysRevB*.23, pp6008 (June 1981).
- [13] SolidWorks is a solid modeling computer-aided design (CAD) and computer-aided engineering (CAE) computer program. The Copyright is owned by SOLIDWORKS Corp, USA.
- [14] Commercial TEM is employed for reference in part, for example, TEM No. TEHP1-12656-0.3 from the manufacturer owned by Thermonamics Electronics (Jiangxi) Corp., Ltd., China.
- [15] D. Liu, A. J. Jin, "multi-stack thermoelectric segmentation and optimization: a computation software", SW copyrights Reg. ID.: 2015SR094544 V1.0, China (2015); D. Liu, A. J. Jin, HNCERI internal report, "The computer simulation with the finite elements method of triple stack TEPG predicts that the efficiency can achieve over 19%", (2013).
- [16] T. S. Ursell, G. J. Snyder, "Compatibility of Segmented Thermoelectric Generators. Twenty-First International Conference on Thermoelectrics", *ICT 200*, pp412–417 (2002).
- [17] G. S. Nolas, J. Sharp, H. J. Goldsmid, "Thermoelectrics-Basic Principles and New Material Developments," Springer publ., Berlin (2001).
- [18] P. M. Solanki, D. S. Deshmukh, D. C. Talele; "A Critical Review on Operating Variables of Solar Thermoelectric Power Generator"; *Pratibha: International Journal of Science, Spirituality, Business and Technology (IJSSBT)*, Vol. 3, No. 2, PP49-54, (June 2015) India.
- [19] L. D. Zhao, Y. Zhang, H. Sun, G. Tan, C. Uher, C. Wolverton, V. P. Dravid& M. G. Kanatzidis (2014), "Ultralow Thermal Conductivity and High Thermoelectric Figure of Merit in SnSe Crystals", *Nature* 508 (7496) 373-377 (Nov., 2014). DOI: <http://dx.doi.org/10.1038/nature13184>.
- [20] J. C. Mills, R. C. Dahlberg, "Thermionic Systems for DOD Missions". *AIP Conference Proceedings*. 217(3): 1088–92 (Jan. 1991) doi: 10.1063/1.40069. G. M. Gryaznov; E. E. Zhabotinskii, A. V. Zrodnikov, Y. V. Nikolaev, N. N. Ponomarev-Stepnoi, V. Ya. Pupko, V. I. Serbin and V. A. Usov, "Thermoemission Reactor-Converters for Nuclear Power Units in Outer Space", *Atomic Energy (translated from AtomnayaĖnergiya)*, Plenus Pub. Co. 66 (6): 374–377 (June 1989). doi: 10.1007/BF01123508.
- [21] S. Li, J. Pei, D. Liu, L. Bao, J. F. Li, H. Wu, L. Li, "Fabrication and characterization of thermoelectric power generators with segmented legs synthesized by one-step spark plasma sintering", *Energy*; vol.113, pp. 35 – 43 (2016).
- [22] A. J. Jin, W. Peng, internal reports, CERI/TW-RA-006-13 (2013) of China Hua-Neng Group. Authors has benefited by numerous discussions with partners, peers, and vendors. They appreciate their supports to meet some aggressive project spec. Some of the VLSI processes provided by J. Chien for thick oxide growth, by G. Yin for patterned etch of thick oxide in AMEC Ltd., and by Prof. T. Deng for the filling of both p-type and n-type BiTe.
- [23] S Khan, L Lorenzelli, R S Dahiya, "Technologies for printing sensors and electronics over large flexible substrates: A review", *IEEE Sens J*, 2014, 15(6): 3164–3185.
- [24] Z Yin, Y Huang, N Bu, et al. "Inkjet printing for flexible electronics: Materials, processes and equipment", *Chinese Science Bull*, 2010, 55(30): 3383–3407.

## Biography



**Dr. A. Jerry Jin** has held positions of the chief scientist in China Huan-neng Group and the adjunct professor in Ningbo Institute of Materials Technology and Materials, ACS. His recent focus is on alternative energies and new materials. He has extensive research experience in EE, material science, and applied physics. Jerry has earned his PhD in applied physics from University of Minnesota. He has held positions in several premier universities and institutes such as Case Western Reserve University and NASA. Dr. Jin is a recipient of the distinguished one-thousand-oversea-talents in China and a senior member of IEEE and PMI.



**Dr Yuanming Zhang** is a professor of additive manufacturing at the Ningbo Institute of Materials Technology and Engineering, Chinese Academy of Sciences. He completed a PhD in Mechanical Engineering from the University of Sheffield in 2006. He has multidisciplinary research and industrial experience in product design and development of a large-scale slurry building, near net shape powder-based manufacturing, and nano-suspension ink-jet for 3D printing technology. He is an executive director of Chinese Materials New Technology Development Research Institute from 2014.